

Birefringence of GaN/AlGaN optical waveguides

R. Hui, Y. Wan, J. Li, S. X. Jin, J. Y. Lin, and H. X. Jiang

Citation: *Applied Physics Letters* **83**, 1698 (2003); doi: 10.1063/1.1606103

View online: <http://dx.doi.org/10.1063/1.1606103>

View Table of Contents: <http://scitation.aip.org/content/aip/journal/apl/83/9?ver=pdfcov>

Published by the [AIP Publishing](#)

Articles you may be interested in

[Birefringence and refractive indices of wurtzite GaN in the transparency range](#)

Appl. Phys. Lett. **107**, 092104 (2015); 10.1063/1.4929976

[GaN-based waveguide devices for long-wavelength optical communications](#)

Appl. Phys. Lett. **82**, 1326 (2003); 10.1063/1.1557790

[Interface properties of Al x Ga 1-x N/AlN heterostructures from optical waveguiding information](#)

Appl. Phys. Lett. **75**, 3324 (1999); 10.1063/1.125339

[Optical properties of low-pressure metalorganic vapor phase epitaxy Al x Ga 1-x N thin-film waveguides by prism coupling technique](#)

Appl. Phys. Lett. **74**, 3960 (1999); 10.1063/1.124236

[Phase-matched optical second-harmonic generation in GaN and AlN slab waveguides](#)

J. Appl. Phys. **85**, 2497 (1999); 10.1063/1.369611

The advertisement for MMR Technologies features a blue and red color scheme. On the left is the MMR Technologies logo. The main text reads 'THE WORLD'S RESOURCE FOR VARIABLE TEMPERATURE SOLID STATE CHARACTERIZATION'. Below this text are five images of different measurement systems: Optical Studies Systems, Seebeck Studies Systems, Microprobe Stations, Hall Effect Study Systems and Magnets, and a large magnet assembly. The website address www.mmr-tech.com is at the bottom left.

MMR
TECHNOLOGIES

**THE WORLD'S RESOURCE FOR
VARIABLE TEMPERATURE
SOLID STATE CHARACTERIZATION**

[WWW.MMR-TECH.COM](http://www.mmr-tech.com)

OPTICAL STUDIES SYSTEMS SEEBECK STUDIES SYSTEMS MICROPROBE STATIONS HALL EFFECT STUDY SYSTEMS AND MAGNETS

Birefringence of GaN/AlGaN optical waveguides

R. Hui^{a)} and Y. Wan

Department of Electrical Engineering and Computer Science, The University of Kansas, Lawrence, Kansas 66044

J. Li, S. X. Jin, J. Y. Lin, and H. X. Jiang

Department of Physics, Kansas State University, Manhattan, Kansas 66506-2601

(Received 9 April 2003; accepted 1 July 2003)

We have experimentally studied the birefringence of wurtzite GaN grown on a sapphire substrate. The measurements were done with single-mode GaN/AlGaN planar optical waveguides on *c*-plane grown heterostructure films. The refractive indices were found to be different for signal optical field perpendicular or parallel to the crystal *c* axis ($n_{\perp} \neq n_{\parallel}$). More importantly, we found an approximately 10% change in index difference $\Delta n = n_{\parallel} - n_{\perp}$ with variation of the waveguide orientation in the *a*-*b* plane, and a 60° periodicity was clearly observed. This is attributed to the hexagonal structure of nitride materials. © 2003 American Institute of Physics. [DOI: 10.1063/1.1606103]

Wide band gap III-nitride semiconductor material plays an increasingly important role in the development of light emitting devices in the blue and ultraviolet wavelength regions.¹⁻³ In addition, with the rapid advancement of photonic integrated circuits, III-nitride optical waveguide devices have also been suggested for application in long wavelength optical communication windows as switchable optical phasors.⁴ In both applications, the refractive index of the material is a critical parameter in waveguide design and device performance. The birefringence of GaN films grown on sapphire substrates has been reported⁵ where a refractive index change of approximately 4% was observed in the long wavelength region (around 800 nm) when the signal polarization was switched from perpendicular to parallel to the crystal *c* axis.⁶ On the other hand, the crystal lattice of GaN has a hexagonal configuration on the plane (*a*-*b* plane) perpendicular to the *c* axis. It has been shown that the efficiency of optical emission changed periodically when the optical propagation direction was varied in the *a*-*b* plane.⁷ Since this anisotropic emission efficiency is caused by the wurtzite structure of the crystal lattice, anisotropy of the refractive index in the *a*-*b* plane may also exist. This later effect is especially important for passive optical waveguide design. In this work, we investigate the birefringence in single-mode GaN/AlGaN optical waveguides operating in the 1550 nm optical communication wavelength region. We demonstrate that the refractive index not only depends on the signal polarization states (parallel or perpendicular to the *c* axis), it also depends on the direction of optical propagation in the *a*-*b* plane.

In order to perform this investigation, single-mode ridged optical waveguides were designed by a beam-propagation method (BPM) simulation tool. Figure 1 shows schematically the cross section of the optical waveguide designed based on the GaN core, Al_xGa_{1-x}N cladding and a sapphire substrate. According to our BPM simulation, this waveguide is single mode for $\lambda > 1.1 \mu\text{m}$. The waveguide

structure was grown by metalorganic chemical vapor deposition (MOCVD) on the *c* plane of sapphire. A 4- μm -thick epitaxial film of Al_xGa_{1-x}N ($x = 0.03$) was grown first followed by a 3- μm -thick GaN film deposited on top of the Al_xGa_{1-x}N layer. Then optical waveguides were fabricated by photolithographic patterning and inductively coupled plasma (ICP) dry etching. According to the design, the etching depth is controlled at approximately 2.8 μm and the waveguide width is 3 μm . In order to investigate the birefringence effect as a function of the wave propagation direction, a number of waveguide samples were prepared each with a different orientation angle θ with respect to the *a* axis in the *a*-*b* plane. The lengths of the waveguide samples ranged from 1.5 to 3 mm. The waveguide end surfaces were cut so as to be perpendicular to the propagation direction *G*.

Our experiment was based on measurement of the Fabry-Pérot (FP) interference caused by Fresnel reflections from the two end facets of the waveguide. The effective refractive index can be precisely determined by measurement of the FP transfer function. To characterize these waveguide samples, a fiberoptic setup operating in the 1550 nm wavelength region was used. An erbium-doped fiber amplifier

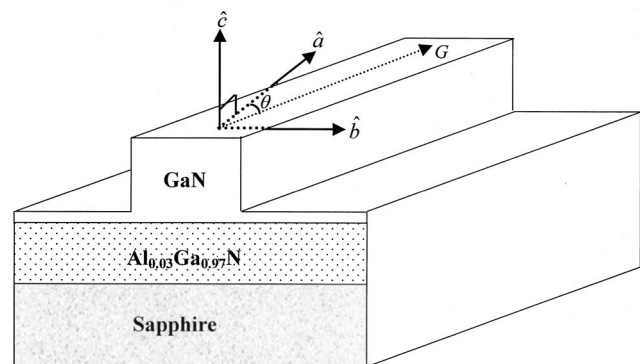


FIG. 1. Schematic illustration of the waveguide cross section and wave propagation direction *G* with respect to the GaN crystal structure in Cartesian coordinates ($c \perp a \perp b$). Waveguide orientation angle θ is defined as the angle between *G* and *a* in the *a*-*b* plane.

^{a)}Electronic mail: hui@eecs.ukans.edu

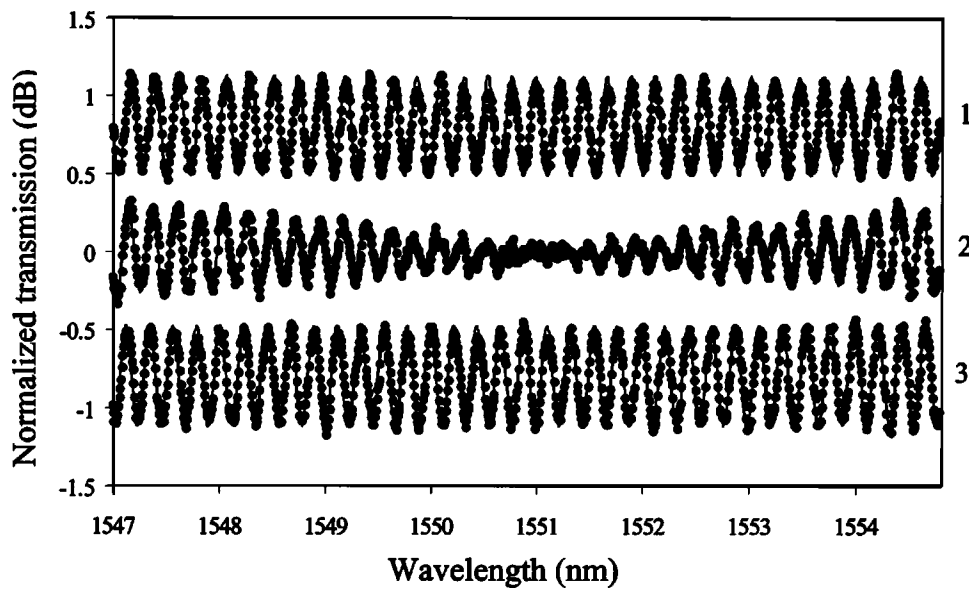


FIG. 2. Measured (closed circles) and calculated (continuous lines) optical transfer functions with the input optical field perpendicular (trace 1), parallel (trace 3) and 45° from (trace 2) the crystal c axis.

(EDFA) without optical signal input was used in this measurement and it provides wideband amplified spontaneous emission (ASE). To evaluate the polarization effect, a fiber-optical polarizer was used immediately behind the wideband ASE source and a polarization controller was inserted behind the polarizer to adjust the signal polarization before it is injected into the waveguide sample. Optical coupling at the input and the output of the waveguide was accomplished by using tapered single-mode fibers with 6 μm working distance and a 2.5 μm spot size of focus. Each tapered fiber end was mounted on a five-dimensional precision positioning stage to optimize the optical coupling efficiency. An optical spectrum analyzer was used to measure the ASE optical spectrum after it passed through the optical waveguide sample. Then the transfer function of the optical waveguide can be obtained by comparing the output spectrum with that at the input.

Figure 2 shows an example of the measured optical transfer functions on a waveguide sample. This particular waveguide is oriented at an angle of $\theta=15^\circ$ with respect to the a axis of the crystal. The three traces in Fig. 2 represent the transfer functions measured at three different optical signal polarization states. Trace 1 has the input optical signal polarized perpendicular to the c axis while trace 3 has the signal parallel to the c axis. The average values of the transfer functions shown were intentionally shifted ± 0.8 dB for the purpose of better display. Regular FP-like transfer functions are clearly seen in both of these two traces with only a slight difference in their period. Despite some minor contrast variations caused by the random noise and mechanical vibrations in the measurement setup, these two measured traces can be numerically fit by a normalized FP transfer function:

$$T(\lambda) = \left\{ 1 + R^2 - 2R \cos \left[\frac{4\pi L(n_{\text{eff}} \pm \Delta n/2)}{\lambda} + \varphi_0 \right] \right\}^{-1}, \quad (1)$$

where $L=2.31$ mm is the waveguide length, which is measured by moving the waveguide under a microscope using a precision translational stage with 1 μm resolution. $R=3.75\%$

is the effective roundtrip power loss of the waveguide including mirror loss at the waveguide end surface due to Fresnel reflection and facet tilt caused by the cutting error. In practice, the facet tilt reduces the effective reflectivity and thus reduces the contrast in FP fringes in the experiments. φ_0 is an initial phase and n_{eff} is the effective refractive index of the waveguide, which can be determined by best fitting between the measured and the calculated FP fringe period. Strictly speaking, the effective index obtained by this measurement is the *group index* because the dispersion effect is automatically included. However, since the measurement was performed in the 1550 nm wavelength region, which is far from the material band gap, the dependence of the refractive index on the wavelength is very weak. In fact, within a 10 nm measurement wavelength region in the vicinity of 1550 nm, the index change is less than 10^{-4} (Ref. 4) so the dispersion effect is neglected in this letter.

If we consider the effect of birefringence, the effective refractive index is $n_{\text{eff}}=n_{\perp}$ if the optical field is perpendicular to the material's c axis and $n_{\text{eff}}=n_{\parallel}$ when the field is parallel to the c axis, where generally $n_{\perp} \neq n_{\parallel}$. The solid lines in Fig. 2 are numerical fits using Eq. (1). To obtain the best fit to the transfer functions measured (closed circles) of traces 1 and 3, refractive indices of $n_{\parallel}=2.357$ and $n_{\perp}=2.315$ were used and thus the value of the birefringence is $\Delta n=(n_{\parallel}-n_{\perp})=0.042$ in this particular case. In order to exclude birefringence which may be caused by the waveguide structure, a separate vectorial BPM simulation was performed by solving the Maxwell equations and computing both \perp and \parallel and G field components. The calculated results indicated that with the waveguide design shown in Fig. 1, the index difference between \perp and \parallel polarization components induced by the waveguide structure, is less than 10^{-5} , which is three orders of magnitude lower than the measured birefringence. Therefore, this Δn value of 0.042 obtained in the measurement is predominantly caused by material birefringence. Trace 2 in Fig. 2 was obtained by splitting the input optical signal equally into \perp and \parallel polarization modes. In this case,

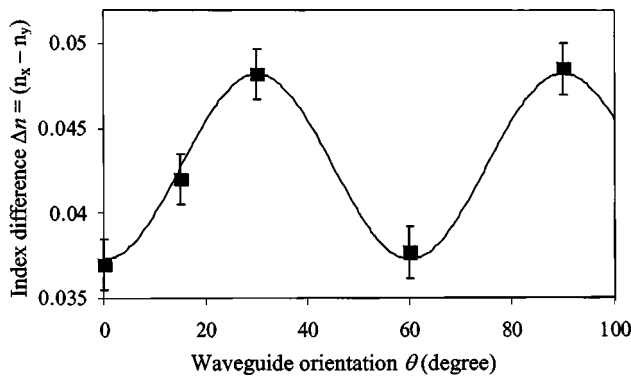


FIG. 3. Measured birefringence $\Delta n = (n_{\parallel} - n_{\perp})$ vs waveguide orientation angle θ in the a - b plane (closed squares). The continuous line is a sinusoid fit using $\Delta n = 0.04275 - 0.00545 \cos(6\theta)$ where θ is in deg.

the ripple amplitude of the FP transfer function has a null at 1551.2 nm. This was because π phase walkoff between the transverse electric (TE) and the transverse magnetic (TM) polarization components happened at that wavelength, and it can be verified by a careful comparison between trace 1 and trace 3 in Fig. 2. We were also able to find multiple nulls in each FP transfer function by enlarging the measurement wavelength coverage. The birefringence can then be easily determined by

$$\Delta n = \lambda_0^2 / (2L\Delta\lambda), \quad (2)$$

where λ_0 is the average wavelength used in the measurement and $\Delta\lambda$ is the difference in wavelength between the adjacent nulls in the transfer function.

A more systematic measurement was then performed by measuring a number of waveguide samples which are oriented at angles of $\theta = 0^\circ, 15^\circ, 30^\circ, 60^\circ,$ and 90° , with respect to the a axis. Figure 3 shows the measured birefringence versus the waveguide orientation angle θ . The birefringence value Δn changed more than 10% by varying the waveguide

orientation angle and, in addition, 60° periodicity was clearly observed. The continuous curve in Fig. 3 is a sinusoid fit using $\Delta n = 0.04275 - 0.00545 \cos(6\theta)$. This anisotropy is most likely caused by the hexagonal crystal structure of GaN. Although the periodic variation of Δn in the a - b plane is measured in infrared wavelengths, we believe this 60° periodicity in Δn variation also exists in wavelength regions near the band edge, where the periodic emission-efficiency variation versus angle θ in the a - b plane has already been reported.⁷

In summary, we have studied the birefringence of GaN/AlGaN planar optical waveguides grown on a sapphire substrate. We have demonstrated that the refractive index not only depends on the signal polarization states parallel or perpendicular to the c axis, it also depends on the direction of optical propagation in the a - b plane. Periodicity of 60° was found for the birefringence change versus the waveguide orientation. This is attributed to the wurtzite structure of GaN crystals.

This work supported by NSF through the Ultra-High-Capacity Optical Communications and Networks (ECS-0123450) and by DMR-0203373.

¹S. Nakamura, M. Senoh, S. Nagahama, N. Iwasa, T. Yamada, T. Matushita, H. Kiyoku, and Y. Sugimoto, *Jpn. J. Appl. Phys., Part 2* **35**, L74 (1996).

²S. Nakamura and G. Fasol, *The blue Laser Diodes* (Springer, Berlin, 1997).

³S. X. Jin, J. Li, J. Z. Li, J. Y. Lin, and H. X. Jiang, *Appl. Phys. Lett.* **76**, 631 (2000).

⁴R. Hui, S. Taherion, Y. Wan, J. Li, S. X. Jin, J. Y. Lin, and H. X. Jiang, *Appl. Phys. Lett.* **82**, 1326 (2003).

⁵V. Fiorentini, F. Bernardini, F. Della Sala, A. Di Carlo, and P. Lugli, *Phys. Rev. B* **60**, 8849 (1999).

⁶S. Ghosh, P. Waltereit, O. Brandt, H. T. Grahn, and K. H. Ploog, *Appl. Phys. Lett.* **80**, 413 (2002).

⁷T. N. Oder, J. Y. Lin, and H. X. Jiang, *Appl. Phys. Lett.* **79**, 12 (2001).